PHYSICAL REVIEW B **80**, 161306(R) (2009)

Exactly solved model for an electronic Mach-Zehnder interferometer

D. L. Kovrizhin[1,2] and J. T. Chalker[1]
[1]*Theoretical Physics, Oxford University, 1 Keble Road, Oxford OX1 3NP, United Kingdom*
[2]*RRC Kurchatov Institute, 1 Kurchatov Sq., Moscow 123182, Russia*
(Received 25 September 2009; published 19 October 2009)

We study nonequilibrium properties of an electronic Mach-Zehnder interferometer built from integer quantum Hall edge states at filling fraction $\nu=1$. For a model in which electrons interact only when they are inside the interferometer, we calculate exactly the visibility and phase of Aharonov-Bohm fringes at finite source-drain bias. When interactions are strong, we show that a lobe structure develops in visibility as a function of bias, while the phase of fringes is independent of bias, except near zeros of visibility. Both features match the results of recent experiments [Neder *et al.*, Phys. Rev. Lett. **96**, 016804 (2006)].

DOI: 10.1103/PhysRevB.80.161306 PACS number(s): 73.43.−f, 71.10.Pm, 42.25.Hz, 73.23.−b

Questions about phase coherence in interacting quantum systems out of equilibrium are of fundamental and wide-ranging importance. Despite great progress over the past decade, many aspects of nonequilibrium problems remain poorly understood. One recent example of this situation is the "unexpected behavior" observed in state-of-the-art experiments on electronic Mach-Zehnder interferometers (MZIs) (Refs. 1–3) driven out of equilibrium by an applied bias voltage. In these experiments the visibility of Aharonov-Bohm (AB) fringes in the conductance shows a lobelike structure as a function of bias, while the phase of oscillations is independent of bias even with different interferometer arm lengths, except at zeros of the visibility where it jumps by π.

These observations have attracted a lot of attention. It was immediately appreciated[1] that they lie outside a single-particle description. Moreover, since integer quantum Hall edge states scale to noninteracting chiral Fermi gases at low energy, the *finite range* of electron-electron interactions seems to be crucial. The effort to understand interaction effects in MZIs at integer filling is therefore linked with work on nonlinear effects in nonchiral Luttinger liquids,[4] as well as to interferometry of fractional quantum Hall quasiparticles.[5] The most obvious consequence anticipated from interactions is dephasing. This may arise from external noise[6] or internally,[7,8] but in both cases is expected to suppress AB fringe visibility smoothly with increasing bias, in contrast to observations. It has been found, however, that zeros in visibility can arise if the edge channels that form the interferometer arms are coupled to another channel: such an extra channel may be a feature of sample design,[9] and is present intrinsically at $\nu=2$.[10] Although those results are encouraging, they do not seem sufficiently universal to explain all current experiments. In this context, two recent papers[11,12] that obtain visibility oscillations from calculations of interaction effects at $\nu=1$ represent an interesting advance. These papers contain illuminating physical insights, and similar phenomena have been shown to exist in another context,[13] but approximations used in Refs. 11 and 12 are not standard ones and their reliability is hard to judge.

In this Rapid Communication we present an exact calculation for a simplified model of an interferometer. It reproduces the main signatures observed experimentally[1–3] and shows that the lobe pattern is a many-body effect, which would not appear in any approximation that treats single particles moving in a static mean-field potential. The model is illustrated in the inset to Fig. 1. As in previous studies, two quantum Hall edge channels, both with the same propagation direction, are coupled at two quantum point contacts (QPCs). The simplifying feature of the model is that electrons interact only when they are *inside* the interferometer. This allows us to combine a description of the contacts using fermion operators with a treatment of interactions using bosonization. Within the MZI we take interactions only between two electrons on the same arm and with fixed strength independent of distance, although it would be feasible to relax these restrictions. We consider an initial state in which Fermi seas in the two channels are filled to different chemical potentials, to represent the bias voltage, and evolve this state forward in time using the Schrödinger equation. At long times the system reaches a stationary regime. In this regime we calculate current and differential conductance as a function of chemical-potential difference and enclosed AB flux. Our main results are presented in Figs. 1 and 2, and discussed following an outline of their derivation; details will be presented elsewhere.[14]

The solution we describe is significant more broadly as a rare example of a solved nonequilibrium scattering problem. One earlier instance is that of tunneling between fractional

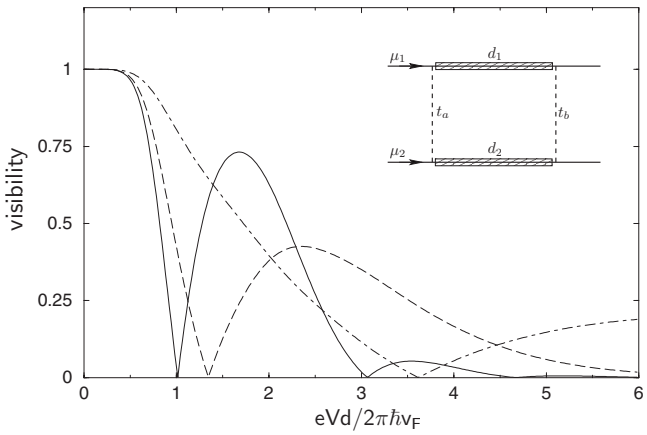

FIG. 1. Visibility as a function of bias voltage for MZI with $d_1=d_2$ and $t_a^2=t_b^2=1/2$ at interaction strengths: $\tilde{\gamma}=1$ (dot-dashed line), $\tilde{\gamma}=2$ (dashed line), and $\tilde{\gamma}=3$ (full line), where $\tilde{\gamma}=2\pi\gamma$. Inset: schematic view of model studied.

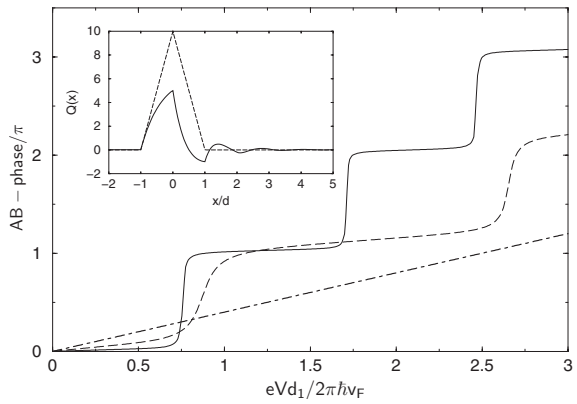

FIG. 2. Dependence of interference fringe phase on bias voltage for MZI with unequal arm lengths, $d_2/d_1=1.2$, at interaction strengths: $\tilde{\gamma}=0$ (dot-dashed line), $\tilde{\gamma}=3$ (dashed line), and $\tilde{\gamma}=10$ (full line). Inset: the kernel $Q(x)$ of Eq. (11) at $\tilde{\gamma}=10$ (full line) and that of Ref. 11 (dashed line).

quantum Hall edge states,[15] while another is the interacting resonant-level model, treated recently by a form of Bethe Ansatz,[16] and using boundary field theory.[17] The remarkable structure observed experimentally[1–3] makes the MZI particularly interesting in this context.

The Hamiltonian $\hat{H}=\hat{H}_{kin}+\hat{H}_{int}+\hat{H}_{tun}$ for the model has three contributions, representing respectively: kinetic energy, interactions, and tunneling at contacts. We formulate $\hat{H}$ initially for edges of length L with periodic boundary conditions, then take the limit $L\to\infty$. Then

$$\hat{H}_{kin}=-i\hbar v_F\sum_{\eta=1,2}\int_{-L/2}^{L/2}\hat{\psi}_\eta^+(x)\partial_x\hat{\psi}_\eta(x)dx, \tag{1}$$

where v_F is the Fermi velocity and $\eta=1,2$ is the channel index. The Fermi field operators can be written as $\hat{\psi}_\eta(x)=L^{-1/2}\Sigma_k\hat{c}_{k\eta}e^{ikx}$, with $k=2\pi n_k/L$ and n_k integer, and $\{\hat{c}_{k\eta},\hat{c}^+_{q\eta'}\}=\delta_{kq}\delta_{\eta\eta'}$. Interactions are described by

$$\hat{H}_{int}=\frac{1}{2}\sum_{\eta=1,2}\int_{-L/2}^{L/2}U_\eta(x,x')\hat{\rho}_\eta(x)\hat{\rho}_\eta(x')dxdx', \tag{2}$$

where $\hat{\rho}_\eta(x)=\hat{\psi}^+_\eta(x)\hat{\psi}_\eta(x)$ is the electron-density operator. In our model $U_\eta(x,x')=0$ for $x,x'\notin(0,d_\eta)$. Finally, the QPCs are represented by

$$\hat{H}_{tun}=v_ae^{i\alpha}\hat{\psi}_1^+(0)\hat{\psi}_2(0)+v_be^{i\beta}\hat{\psi}_1^+(d_1)\hat{\psi}_2(d_2)+\text{H.c.} \tag{3}$$

The AB phase appears here as $\varphi_{AB}\equiv\beta-\alpha$.

The total current I from channel 1 to 2 has contributions I_a and I_b arising from each QPC, which can be written in terms of expectation values of operators acting at points infinitesimally before the QPC. Each contribution can be separated into a term that is not sensitive to coherence between the edges, and another that is sensitive. We define $t_{a,b}=\sin\theta_{a,b}$ and $r_{a,b}=\cos\theta_{a,b}$ with $\theta_{a,b}=v_{a,b}/\hbar v_F$, and denote expectation values by $\langle\ldots\rangle$. A straightforward calculation yields for QPC b the expressions $I_b=I_b^{(1)}+I_b^{(2)}$, with

$$I_b^{(1)}=ev_Ft_b^2\langle\hat{\rho}_1(d_1)-\hat{\rho}_2(d_2)\rangle$$

$$I_b^{(2)}=ev_Ft_br_b[ie^{i\beta}\langle\hat{G}_{12}\rangle+\text{H.c.}],$$

where $\hat{G}_{12}=\hat{\psi}_1^+(d_1)\hat{\psi}_2(d_2)$. Terms in I_a are obtained from these for I_b by replacing d_1 and d_2 with 0, and v_b with v_a. Since there is no coherence between channels before QPC a, $I_a^{(2)}=0$ and the term responsible for AB oscillations in current is $I_b^{(2)}$. The bias voltage is $V=(\mu_1-\mu_2)/e$ and the differential conductance is $\mathcal{G}=e\mathrm{d}I/\mathrm{d}\mu_1$ (with μ_2 fixed). $\mathcal{G}$ oscillates with φ_{AB}, having maximum and minimum values $\mathcal{G}_{\max}$ and $\mathcal{G}_{\min}$, and *AB fringe visibility* is defined as $(\mathcal{G}_{\max}-\mathcal{G}_{\min})/(\mathcal{G}_{\max}+\mathcal{G}_{\min})$.

The central task is therefore to calculate the correlator $\langle\hat{G}_{12}\rangle$, and our approach is as follows. (i) We work in the interaction representation, evolving operators with $\hat{H}_0=\hat{H}_{kin}+\hat{H}_{int}$ and treating $\hat{H}_{tun}$ as the "interaction". Then $\hat{\psi}_\eta(x,t)=e^{i\hat{H}_0t/\hbar}\hat{\psi}_\eta(x)e^{-i\hat{H}_0t/\hbar}$ (note that we distinguish operators in the Schrödinger and interaction representations by the absence or presence of a time argument). The wave function of the system, denoted at $t=0$ by $|Fs\rangle$, evolves with the S-matrix $\hat{S}(t)=\mathrm{T}\exp\{-(i/\hbar)\int_0^t\hat{H}_{tun}(t')dt'\}$, where T indicates time ordering. (ii) Time evolution of operators is calculated using bosonization to diagonalize $\hat{H}_0$. (iii) Results are written in terms of operators in the Schrödinger picture, with boson operators re-expressed using fermion ones. This yields an expression for $\hat{G}_{12}$ suitable for straightforward numerical evaluation. We next outline these three steps.

Step (i): evaluation of $\hat{S}(t)$ hinges on our restriction of interactions to the interior of the MZI. Specifically, separating $\hat{H}_{tun}$ into parts $\hat{H}^a_{tun}$ and $\hat{H}^b_{tun}$ due to each QPC, we find from step (ii) that $[\hat{H}^a_{tun}(t_1),\hat{H}^b_{tun}(t_2)]=0$ and $[\hat{G}_{12}(t_1),\hat{H}^b(t_2)]=0$, provided $t_1\geq t_2$. The first commutator allows us to factorize the S-matrix as $\hat{S}(t)=\hat{S}^b(t)\hat{S}^a(t)$, where $\hat{S}^a(t)$ is calculated using $\hat{H}^a_{tun}$ and $\hat{S}^b(t)$ using $\hat{H}^b_{tun}$. The second ensures that $[\hat{S}^b(t)]^+\hat{G}_{12}(t)\hat{S}^b(t)=\hat{G}_{12}(t)$ so that an explicit form for $\hat{S}^b(t)$ is not required in the calculation. Since QCP a acts before interactions, $\hat{S}^a(t)$ is easy to evaluate: we have $[\hat{H}^a_{tun}(t_1),\hat{H}^a_{tun}(t_2)]=0$ for any $t_1,t_2\geq0$ and so may omit time ordering. In particular, we will need to compute the action of $\hat{S}^a(t)$ on fermionic operators. It is a rotation in the space of channels and can be written $\tilde{\hat{\psi}}_\eta(x)=[\hat{S}^a(t)]^+\hat{\psi}_{\eta'}(x)\hat{S}^a(t)$. For $0<x<v_Ft$ we find

$$\tilde{\hat{\psi}}_\alpha(x)=\sum_\beta\mathcal{S}^a_{\alpha\beta}\hat{\psi}_\beta(x),$$
$$\mathcal{S}^a=\begin{pmatrix}r_a & -it_ae^{i\alpha}\\ -it_ae^{-i\alpha} & r_a\end{pmatrix}. \tag{4}$$

Step (ii): we compute time evolution under $\hat{H}_0$ using bosonization.[18] Fermion operators are written in the form

$$\hat{\psi}_\eta(x)=(2\pi a)^{-1/2}\hat{F}_\eta e^{i2\pi/L\hat{N}_\eta x}e^{-i\hat{\phi}_\eta(x)}, \tag{5}$$

where $\hat{F}_\eta$ are Klein factors with commutation relations $\{\hat{F}_\eta,\hat{F}^+_{\eta'}\}=2\delta_{\eta\eta'}$ and bosonic fields are defined as

$$\hat{\phi}_\eta(x) = -\sum_{q>0} (2\pi/qL)^{1/2}(e^{iqx}\hat{b}_{q\eta} + \text{H.c.})e^{-qa/2}, \quad (6)$$

with a an infinitesimal regulator. Plasmon creation operators obey bosonic commutation relations $[\hat{b}_{q\eta}, \hat{b}^+_{k\eta'}] = \delta_{qk}\delta_{\eta\eta'}$ and are expressed for $q>0$ in terms of fermions as

$$\hat{b}^+_{q\eta} = i(2\pi/qL)^{1/2} \sum_{k=-\infty}^{\infty} \hat{c}^+_{k+q\eta}\hat{c}_{k\eta}. \quad (7)$$

Since $\hat{H}_0$ does not couple channels, we restrict attention to a single channel and omit channel labels until we reach step (iii). The kinetic energy $\hat{H}_{kin}$ for a single edge has the bosonized form

$$\hat{H}_{kin} = \frac{\hbar v_F}{2}\int_{-L/2}^{L/2} \frac{dx}{2\pi}(\partial_x\hat{\phi}(x))^2 + \frac{2\pi}{L}\frac{\hbar v_F}{2}\hat{N}(\hat{N}+1) \quad (8)$$

where $\hat{N} \equiv \Sigma_k \hat{c}^+_k \hat{c}_k$ is the particle number operator. Similarly, $\hat{H}_{int}$ is quadratic when written using the bosonic representation of the density operators, $\hat{\rho}(x) = -\frac{1}{2\pi}\partial_x\hat{\phi}(x) + \hat{N}/L$. The time dependence of $\hat{\phi}(x,t)$ can be found by solving the equation of motion. Since our choice of nonuniform interactions leads to a coupling between the plasmon and number operators, we make the separation $\hat{\phi}(x,t) = \hat{\phi}^{(0)}(x,t) + \hat{\phi}^{(1)}(x,t)$, where $\hat{\phi}^{(0)}(x,t) \propto \hat{N}/L$ and $\hat{\phi}^{(1)}(x,t)$ is independent of $\hat{N}$, satisfying

$$2\pi\hbar(\partial_t + v_F\partial_x)\hat{\phi}^{(1)}(x,t) = -\int U(x,y)\partial_y\hat{\phi}^{(1)}(y,t)\mathrm{d}y. \quad (9)$$

The solution can be written in the form

$$\hat{\phi}^{(1)}(x,t) = \int_{-L/2}^{L/2} K(x,y;t)[\hat{\phi}(y) - \hat{\phi}^{(0)}(y)]\mathrm{d}y,$$

where the Green's function $K(x,y;t)$ can be constructed in the usual way from the eigenfunctions of the time-independent equation,

$$2\pi\hbar v_F(\partial_x - ip)f_p(x) = -\int U(x,y)\partial_y f_p(y)\mathrm{d}y.$$

We now specialize to interactions that are constant within the interferometer: $U(x,x') = g$ for $x,x' \in (0,d)$ and $U(x,x') = 0$ otherwise. This form of the potential is the one treated approximately in.[11] It is characterized by the dimensionless coupling constant $\gamma = gd/2\pi\hbar v_F$. We find in the limit $L \to \infty$

$$f_p(x) = \begin{cases} e^{ipx} & x \le 0 \\ r_p + s_p e^{ipx} & 0 < x < d \\ e^{ipx - i\delta_p} & x \ge d \end{cases}.$$

The coefficients $s_p = (1+t_p)^{-1}$ and $r_p = t_p s_p$, with $t_p = (i\gamma/pd)(1-e^{ipd})$, are obtained from matching $f_p(x)$ at $x = 0, d$. The phase shifts of plasmons δ_p due to the interactions are given by $e^{-i\delta_p} = (1+t^*_p)/(1+t_p)$. Similarly, we find $\hat{\phi}^{(0)}(x) = 2\pi\bar{\gamma}\hat{N}x/L$ for $x \in (0,d)$, where $\bar{\gamma} = \gamma(1+\gamma)^{-1}$.

In this way we find an expression for $K(x,y;t)$. Setting $x=d$, it simplifies at long times to

$$K(d,y;t) = \frac{1}{2\pi}\int_{-\infty}^{\infty} dp e^{i(p[d-y-v_F t]-\delta_p)}. \quad (10)$$

Using this and Eqs. (6) and (7), we write $\hat{\phi}^{(1)}(x,t)$ as a bilinear in the fermion operators $\hat{c}^+_k$ and $\hat{c}_k$.

Step (iii): We employ this result to construct an expression for $\hat{G}_{12}(t)$ in terms of fermion operators in the Schrödinger representation. To this end, we start from Eq. (5) in the interaction representation at time t and substitute for $\hat{\phi}_\eta(d_\eta,t)$ as described. We also eliminate the combination $\mathcal{F} \equiv (2\pi a)^{-1/2}\hat{F}_\eta e^{i2\pi/L\hat{N}_\eta d_\eta}$ by inverting the bosonization identity, Eq. (5), writing

$$\mathcal{F}(t) = e^{i\hat{H}_{kin}t/\hbar}\mathcal{F}e^{-i\hat{H}_{kin}t/\hbar} = \hat{\psi}_\eta(z)e^{i\hat{\phi}_\eta(z)}$$

for $z_\eta = d_\eta - v_F t$. Finally, we substitute for $\hat{b}_{q\eta}$ and $\hat{b}^+_{q\eta}$ in $\hat{\phi}_\eta(x)$ using Eq. (7). The result (omitting an unimportant, constant phase) is the operator identity

$$\hat{\psi}_\eta(d_\eta,t) = e^{-i\hat{Q}_\eta}\hat{\psi}_\eta(z_\eta). \quad (11)$$

Here $\hat{Q}_\eta = \int_{-\infty}^{\infty} Q_\eta(x-z_\eta)\hat{\rho}_\eta(x)dx$, where the kernel $Q_\eta(x) = L^{-1}\Sigma_{q=-\infty}^{\infty}\tilde{Q}_\eta(q)e^{iqx}$ has for our choice of interaction the Fourier transform

$$\tilde{Q}_\eta(q) = 2\pi\gamma d_\eta j_0^2(qd_\eta/2)(1 + \gamma e^{-iqd_\eta/2}j_0(qd_\eta/2))^{-1} \quad (12)$$

in which $j_0(x) = x^{-1}\sin x$.

In this way we arrive at the expression

$$\langle G_{12}(t)\rangle = e^{i\bar{\Phi}}\langle Fs|[\hat{S}^a(t)]^+\hat{\psi}^+_1(z_1)e^{i\hat{R}}\hat{\psi}_2(z_2)\hat{S}^a(t)|Fs\rangle.$$

Here $\bar{\Phi}$ is an initial phase that is independent of voltage, and $\hat{R} = \hat{Q}_1 - \hat{Q}_2$. The action of $\hat{S}^a(t)^+$ and $\hat{S}^a(t)$ on the operators they enclose is given by Eq. (4), and evaluation of $\langle\hat{G}_{12}(t)\rangle$ reduces to the calculation of correlators of the form $C_{\mu\eta} = \langle Fs|\hat{c}^+_\mu \exp(i\Sigma_{\alpha\beta}\mathrm{M}_{\alpha\beta}\hat{c}^+_\alpha\hat{c}_\beta)c_\eta|Fs\rangle$, where the indices specify both channel and momentum, and the matrix M is obtained from $[\hat{S}^a(t)]^+\hat{R}\hat{S}^a(t)$. One can show that $C_{\mu\eta} = \mathrm{D}^{-1}_{\eta\mu}$ det D with D constructed from the matrix elements of $\exp(i\mathrm{M})$ between the single-particle states that are occupied in the Slater determinant $|Fs\rangle$. We calculate $C_{\mu\eta}$ numerically, achieving convergence of the results when keeping up to 10^3 basis states and 400 particles in each channel.

The physical interpretation of the solution we have presented is as follows. Each electron passing QPC b at time t has an accumulated phase from its interactions with other electrons. The phase is a collective effect and is represented by the operator $\hat{Q}_\eta$ in Eq. (11). Contributions from interactions with particles at a distance x from the one at QPC b have a weight determined by the kernel $Q_\eta(x)$, illustrated in the inset to Fig. 2. This weight is largest near $x=0$, showing that interactions with nearby electrons are most important. Moreover, since $Q_\eta(x) = 0$ for $x < -d_\eta$, a given electron is uninfluenced by the ones behind, that enter the interferometer after it exits. The precise form of the kernel reflects the

full many-body physics of the problem: a similar kernel appears in Eq. (11) of Ref. 11 but with a simpler form because of the approximations employed there.

A consequence of the phase $\hat{Q}_\eta$ is that many-particle interference influences the MZI conductance. As an illustration, consider the quantum amplitudes for two particles to pass through the interferometer on all possible paths connecting given initial and final states. Paths for which both particles propagate on the same arm of the interferometer have an interaction contribution to their phase that varies with their separation and is absent if the two particles propagate on different arms. Destructive interference between paths with different interaction phases generates the observed lobe structure.

We now turn to our results. The parameters in the model are: the dimensionless interaction strength γ, the transmission probabilities t_a^2 and t_b^2, the ratio d_2/d_1 of arm lengths, and the dimensionless bias voltage $eV\sqrt{d_1 d_2}/2\pi\hbar v_F$. We consider $1 \leq 2\pi\gamma \leq 10$, $1 \leq d_2/d_1 \leq 1.2$ and first discuss behavior with $t_a^2 = t_b^2 = 1/2$.

The dependence of visibility of AB fringes on bias voltage and interaction strength is presented in Fig. 1, taking equal arm lengths and transmission probabilities of 1/2 at both QPCs. The key features of all three curves in this figure match those of the experiment (see Figs. 2 and 3 of 1): with increasing bias there is a sequence of lobes in the visibility, which have decreasing amplitude and are separated by zeros. The phase of AB fringes is also influenced by interactions. Results are displayed in Fig. 2. For an MZI with different arm lengths (as in this figure), the fringe phase without interactions varies linearly with bias, because the Fermi wavevector k_F is linear in bias and the phase difference between particles traversing the two arms is $k_F(d_2-d_1)$. With increasing interaction strength the phase dependence on bias develops into a series of smooth steps, each of height π. The risers of these steps coincide with minima of the visibility. Strikingly, with strong interactions phase steps at minima of the visibility persist for $d_1=d_2$, even though in this case phase would be independent of bias without interactions. The stepwise phase variation we find at large interaction strength also matches observations (see Fig. 2 of 1).

Behavior is insensitive to the transmission probability t_b^2 at QPC b, apart from the overall scale for visibility. Departures from $t_a^2=1/2$, however, eliminate the exact zeros in visibility, leaving only sharp minima. A difference in arm lengths has a similar though much weaker effect.

The width in bias voltage of the central visibility lobe defines an energy scale. In our model this scale is of order g at large γ. Taking $v_F = 2.5\times 10^4$ ms^{-1}, $d=10$ μm and the permittivity $\epsilon=12.5$ of GaAs, we estimate from the capacitance of an edge channel $g \sim 10$ μeV. This is similar to the experimentally observed value of about 14 μeV.[1]

Our calculations rely on a simplified form for interactions, but we believe our choice is quite reasonable. Our central approximation is to neglect interactions between an electron inside the MZI and one outside. In practice, such interactions will anyway be screened by the metal gates that define the QPCs. We also neglect interactions between a pair of electrons that are both outside the MZI. This is unimportant: before electrons reach the MZI, such interactions do not cause scattering because of Pauli blocking, while after electrons pass through the MZI, these interactions cannot affect the current. Within the MZI we represent interactions by a capacitative charging energy. Such a choice is standard in the theory of quantum dots and has been applied previously to interferometers.[7,11]

In summary, we have calculated the visibility of Aharonov-Bohm fringes in the differential conductance of an electronic MZI out of equilibrium, taking exact account of interactions between electrons. From our calculations we obtain a lobe pattern in the dependence of visibility on bias, and jumps in the phase of fringes at zeros of the visibility, as observed experimentally.[1–3]

We thank F. H. L. Essler for fruitful discussions and acknowledge support from EPSRC-GB (Grants No. EP/D066379/1 and No. EP/D050952/1).

[1] I. Neder, M. Heiblum, Y. Levinson, D. Mahalu, and V. Umansky, Phys. Rev. Lett. **96**, 016804 (2006).
[2] P. Roulleau, F. Portier, D. C. Glattli, P. Roche, A. Cavanna, G. Faini, U. Gennser, and D. Mailly, Phys. Rev. B **76**, 161309(R) (2007).
[3] E. Bieri, M. Weiss, O. Göktas, M. Hauser, C. Schönenberger, and S. Oberholzer, Phys. Rev. B **79**, 245324 (2009).
[4] A. Imambekov and L. I. Glazman, Science **323**, 228 (2009).
[5] C. de C. Chamon, D. E. Freed, S. A. Kivelson, S. L. Sondhi, and X. G. Wen, Phys. Rev. B **55**, 2331 (1997); F. E. Camino, W. Zhou, and V. J. Goldman, *ibid.* **72**, 075342 (2005); K. T. Law, D. E. Feldman, and Y. Gefen, *ibid.* **74**, 045319 (2006); D. E. Feldman and A. Kitaev, Phys. Rev. Lett. **97**, 186803 (2006); V. V. Ponomarenko and D. V. Averin, Phys. Rev. Lett. **99**, 066803 (2007).
[6] F. Marquardt and C. Bruder, Phys. Rev. Lett. **92**, 056805 (2004).
[7] G. Seelig and M. Büttiker, Phys. Rev. B **64**, 245313 (2001).
[8] J. T. Chalker, Y. Gefen, and M. Y. Veillette, Phys. Rev. B **76**, 085320 (2007).
[9] E. V. Sukhorukov and V. V. Cheianov, Phys. Rev. Lett. **99**, 156801 (2007).
[10] I. P. Levkivskyi and E. V. Sukhorukov, Phys. Rev. B **78**, 045322 (2008).
[11] I. Neder and E. Ginossar, Phys. Rev. Lett. **100**, 196806 (2008).
[12] S.-C. Youn, H.-W. Lee, and H.-S. Sim, Phys. Rev. Lett. **100**, 196807 (2008).
[13] B. Abel and F. Marquardt, Phys. Rev. B **78**, 201302(R) (2008).
[14] D. L. Kovrizhin and J. T. Chalker (unpublished).
[15] P. Fendley, A. W. W. Ludwig, and H. Saleur, Phys. Rev. Lett. **75**, 2196 (1995).
[16] P. Mehta and N. Andrei, Phys. Rev. Lett. **96**, 216802 (2006).
[17] E. Boulat, H. Saleur, and P. Schmitteckert, Phys. Rev. Lett. **101**, 140601 (2008).
[18] See: J. von Delft and H. Schoeller, Ann. Phys. **7**, 225 (1998); T. Giamarchi, *Quantum Physics in One Dimension* (Oxford University Press, Oxford, 2004).